Inorg. Chem. **2005**, *44*, 8407−8417

Revisiting the Electronic Structure of Phosphazenes

Adrian B. Chaplin,*,† John A. Harrison,‡ and Paul J. Dyson†

Institut des Sciences et Ingénierie Chimiques, Ecole Polytechnique Fédérale de Lausanne (EPFL), CH-1015 Lausanne, Switzerland, and Department of Chemistry, Institute of Fundamental Sciences, Massey University at Auckland, Private Bag 102 904, North Shore Mail Center, Auckland, New Zealand

Received July 7, 2005

Natural bond orbital (NBO) and topological electron density analyses have been used to investigate the electronic structure of phosphazenes $[N_3P_3R_6]$ (R = H, F, Cl, Br, CH_3, CF_3, $N(C_2H_4)$; 2R = $O_2C_6H_4$), $[N_4P_4Cl_8]$, and $H[NPCl_2]_4H$. Using the former, the two most likely phosphazene bonding alternatives, negative hyperconjugation and ionic bonding have been critically evaluated. Ionic bonding, as suggested by topological analysis, was found to be the dominant bonding feature, although contributions from negative hyperconjugation are necessary for a more complete bonding description. Substituent effects on the P–N bond have been assessed and cases of bond length alternation have been rationalized using this combined bonding model, which supersedes previous models involving d-orbital participation, leading to an explanation for the observed bond length alternation found in some linear polyphosphazenes. In addition, common aromaticity indicators, nucleus independent chemical shifts (NICS) and para-delocalization indices (PDI), have been determined for the cyclophosphazenes.

1. Introduction

The P−N bond is among one of the most intriguing bonds in chemistry and is the building block for a large number of different P, N-based compounds.[1] Phosphazenes (Chart 1) are probably the best known and most extensively studied of these compounds; they constitute the largest class of inorganic macromolecules known. The rich substitution chemistry at the P center in phosphazenes allows the facile derivatization of the P−N backbone conferring stability from hydrolysis and allowing manipulation of their useful material properties.[2] However, while the thermally robust nature of the P−N scaffold is well recognized, the valence unsaturated P−N bond remains poorly understood.

The P−N bond is characteristically short in phosphazenes (ca. 1.58 Å), relative to those in the analogous valence saturated phosphazanes (ca. 1.77 Å), with the shortest bonds found in compounds with highly electronegative substituents such as fluorine.[3] These short bond lengths, together with the lack of bond length alternation in cyclic phosphazenes and to a lesser extent in polyphosphazenes, are also indicative of multiple-bond character. In the valence bond picture, such multiple bond character is problematic because it formally requires the P centers to be hypervalent. Traditionally, the bonding in phosphazenes has been interpreted using Dewar's island model,[4] which states that delocalization occurs via $d\pi_P-p\pi_N$ overlaps resulting in "islands" of electron density over P−N−P units with nodes at the P centers, and is typical of early bonding models which invoke virtual d-orbital

Chart 1

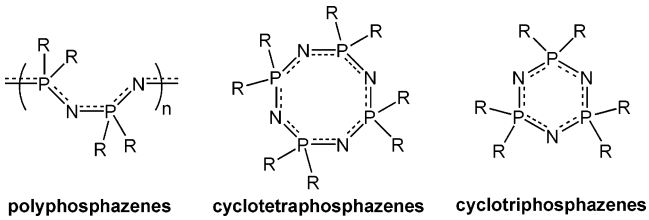

* To whom correspondence should be addressed. E-mail: adrian.chaplin@epfl.ch.
† Ecole Polytechnique Fédérale de Lausanne (EPFL).
‡ Massey University at Auckland.

(1) For examples, see: (a) Shaw, R. A. *Pure Appl. Chem.* **1980**, *52*, 1063−1097. (b) Hauduc, I., Sowerby, D. B., Eds. *The Chemistry of Inorganic Homo- and Heterocycles*; Academic Press: London, 1987; Vol. 2. (c) Corbridge, D. E. C. *Phosphorus: An Outline of its Chemistry, Biochemistry and Technology*, 4th ed.; Elsevier: Amsterdam, 1990. (d) Witt, M.; Roesky, H. W. *Chem. Rev.* **1994**, *94*, 1163−1181.

(2) (a) Allcock, H. R. *Chemistry and Applications of Polyphosphazenes*; Wiley-Interscience: Hoboken, New Jersey, 2003. (b) Gleria, M., De Jaeger, R., Eds. *Phosphazenes: A Worldwide Insight*; Nova Science Publishers: New York, 2004.

(3) (a) Allcock, H. R. *Phosphorus−Nitrogen Compounds: Cyclic, Linear and High Polymeric Systems*; Academic Press: New York, 1972. (b) Allcock, H. R. *Chem. Rev.* **1972**, *72*, 315−356.

(4) Dewar, M. J. S.; Lucken, E. A. C.; Whitehead, M. A. *J. Chem. Soc.* **1960**, 2423−2429.

10.1021/ic0511266 CCC: $30.25
Published on Web 10/13/2005

participation in hypervalent main group elements.[5] However, it is now generally agreed, following accurate ab initio investigations, that valence d orbitals play little role in bonding of the main group elements.[6] Although the incorporation of d-orbital-type basis functions is necessary for the accurate representation of molecular orbitals, they primarily serve as computationally convenient polarization functions.[6]

Instead, it has been suggested that multiple-bond character in hypervalent molecules could be attributed to the presence of negative hyperconjugation,[6] a model pioneered by Reed and Schleyer to describe the bonding in these molecules.[7] In their investigation of molecules with the general formula X_3AY (CF_4, F_3NO, O_3ClF, O_3PS^{3-}, F_3SN, etc.),[7b] they concluded that these molecules contained highly ionic σ bonds with π_{AY} bonding resulting primarily from the interaction of lone pair π_Y orbitals into strongly polarized σ^*_{AX} orbitals, classified as negative hyperconjugation.[8] This proposal has been upheld by recent calculations on a variety of hypervalent molecules[9] and represents one of the most plausible alternatives to Dewar's island model. Despite these findings, the island model still dominates the phosphazene literature, including some recent theoretical investigations of phosphazenes.[10] Other work, based either on Mulliken population analysis[11] or group theory arguments,[12] agrees that the d orbitals appear to be serving as polarization functions, rather than being formally involved in bonding.

Krishnamurthy and co-workers have used the negative hyperconjugation model to rationalize the structures of a number of anomalous phosphazene and phosphazane compounds and, in addition, qualitatively explained that the shortening of the P−N bond with electronegative substituents could result from a more efficient $\pi_N-\sigma^*_{PR}$ overlap.[13] Subsequently, Sun, who performed calculations on a series of phosphazene oligomers, corroborated the negative hyperconjugative model for phosphazenes through a comparison of the electronic structures of H_2NPH_2, HNPH, and $HNPH_3$ calculated at the HF/6-31G* level of theory.[14] Sun concluded that the P−N σ bond in $HNPH_3$ was highly polarized, with a π bond induced largely by electron donation from the π_N to the σ^*_{PH} orbital, with insignificant d_P orbital participation.

Furthermore, a recent topological analysis of the electron density of cyclotriphosphazenes is suggestive of a strong, largely ionic, phosphazene bond,[15] indicating that one of the earliest phosphazene models, the zwitterionic model,[3a] may be more representative of the bonding, although this does not preclude the presence of negative hyperconjugation.

Because of the paucity of theoretical investigations of both the zwitterionic and the negative hyperconjugation models for phosphazenes, we have carried out the first systematic molecular-orbital investigation to evaluate their validity for rationalizing the bonding in phosphazenes. In particular, this work focuses on the cyclotriphosphazenes which are not only computationally, but also chemically, valuable models for the polyphosphazenes. These compounds, isoelectronic with benzene, are also compelling as candidates that might contain inorganic aromaticity and, in this sense, epitomise the controversy surrounding delocalization in phosphazenes.

2. Computational Methods

All geometry optimizations and frequency calculations were carried out using the Gaussian98 suite of programs.[16] After initial tests using $[N_3P_3Cl_6]$ (see Supporting Information, Table S-1), density functional theory, using the hybrid B3LYP functional, was used for all further geometry optimizations and frequency calculations.[17] In general, a pruned grid consisting of 75 radial shells and 302 angular points was used for the calculations, although for $H[NPCl_2]_4H$ a finer grid with 99 radial shells and 590 angular points was necessary. The 6-311++G(2d,2p) basis set was used for all atoms in $[N_3P_3H_6]$, $[H_2NPH_2]$, $[HNPH_3]$, [HNPH], $[HNPCl_3]$, and C_6H_6. For the remaining molecules, the 6-311+G(2d) basis set was used for N, P, and those atoms directly bonded to phosphorus, X, with 6-31G(d,p) used for all other atoms. All of the structures were optimized without imposing symmetry constraints (with the exception of C_6H_6, optimized in D_{6h}) and the resulting geometries were verified as minima by frequency calculations. Optimized geometries are included in the Supporting Information (Table S-2). Important geometrical parameters are summarized in Table 1 and Figure 1.

Nucleus independent chemical shifts (NICS) were computed according to the procedure of Schleyer and co-workers;[18] the magnetic shielding tensor was calculated for a ghost atom located

(5) Mitchell, K. A. R. *Chem. Rev.* **1969**, *69*, 157−178.
(6) (a) Magnusson, E. *J. Am. Chem. Soc.* **1993**, *115*, 1051−1061. (b) Korkin, A. A. *Russ. Chem. Rev.* **1992**, *61*, 473−483. (c) Gilheany, D. G. *Chem. Rev.* **1994**, *94*, 1339−1374 and references therein.
(7) (a) Reed, A. E.; Schleyer, P. v. R. *Inorg. Chem.* **1988**, *27*, 3969−3987. (b) Reed, A. E.; Schleyer, P. v. R. *J. Am. Chem. Soc.* **1990**, *112*, 1434−1445.
(8) Schleyer, P. v. R.; Kos, A. J. *Tetrahedron* **1983**, *39*, 1141−1150.
(9) (a) Kocher, N.; Leusser, D.; Murso, A.; Stalke, D. *Chem.—Eur. J.* **2004**, *10*, 3622−3631. (b) Kormos, B. L.; Cramer, C. J. *Inorg. Chem.* **2003**, *42*, 6691−6700. (c) Chesnut, D. B. *J. Phys. Chem. A* **2003**, *107*, 4307−4313. (d) Dobado, J. A.; Martínez-García, H.; Molina, J. M.; Sundberg, M. R. *J. Am. Chem. Soc.* **2000**, *122*, 1144−1149. (e) Chesnut, D. B. *Heteroat. Chem.* **2000**, *11*, 341−352. (f) Mo, Y.; Zhang, Y.; Gao, J. *J. Am. Chem. Soc.* **1999**, *121*, 5737−5742.
(10) (a) Sabzyan, H.; Kalantar, Z. *Theochem* **2003**, *663*, 149−157. (b) Jaeger, R.; Debowski, M.; Manners, I.; Vancso, G. J. *Inorg. Chem.* **1999**, *38*, 1153−1159. (c) Breza, M. *Theochem* **1998**, *454*, 77−81. (d) Breza, M. *Theochem* **1998**, *429*, 111−120. (e) Breza, M.; Biskupiè, S. *Theochem* **1995**, *332*, 277−281.
(11) Enlow, M. *Polyhedron* **2003**, *22*, 473−482.
(12) (a) Breza, M. *Theochem* **2000**, *505*, 169−177. (b) Breza, M. *Polyhedron* **2000**, *19*, 389−397.
(13) (a) Krishnamurthy, S. S. *Phosphorus, Sulfur Silicon Relat. Elem.* **1994**, *87*, 101−111. (b) Murugavel, R.; Kumaravel, S. K.; Krishnamurthy, S. S.; Nethaji, M.; Chandrasekhar, J. *J. Chem. Soc., Dalton Trans.* **1994**, 847−852.
(14) Sun, H. *J. Am. Chem. Soc.* **1997**, *119*, 3611−3618.
(15) Luaña, V.; Pendás, A. M.; Costales, A.; Carriedo, G. A.; García-Alonso, F. J. *J. Phys. Chem. A* **2001**, *105*, 5280−5291.
(16) Frisch, M. J.; Trucks, G. W.; Schlegel, H. B.; Scuseria, G. E.; Robb, M. A.; Cheeseman, J. R.; Zakrzewski, V. G.; Montgomery, J. A., Jr.; Stratmann, R. E.; Burant, J. C.; Dapprich, S.; Millam, J. M.; Daniels, A. D.; Kudin, K. N.; Strain, M. C.; Farkas, O.; Tomasi, J.; Barone, V.; Cossi, M.; Cammi, R.; Mennucci, B.; Pomelli, C.; Adamo, C.; Clifford, S.; Ochterski, J.; Petersson, G. A.; Ayala, P. Y.; Cui, Q.; Morokuma, K.; Malick, D. K.; Rabuck, A. D.; Raghavachari, K.; Foresman, J. B.; Cioslowski, J.; Ortiz, J. V.; Stefanov, B. B.; Liu, G.; Liashenko, A.; Piskorz, P.; Komaromi, I.; Gomperts, R.; Martin, R. L.; Fox, D. J.; Keith, T.; Al-Laham, M. A.; Peng, C. Y.; Nanayakkara, A.; Gonzalez, C.; Challacombe, M.; Gill, P. M. W.; Johnson, B. G.; Chen, W.; Wong, M. W.; Andres, J. L.; Head-Gordon, M.; Replogle, E. S.; Pople, J. A. *Gaussian 98*, revision A.11.4; Gaussian, Inc.: Pittsburgh, PA, 1998.
(17) (a) Becke, A. D. *Phys. Rev. A* **1988**, *38*, 3098−3100. (b) Becke, A. D. *J. Chem. Phys.* **1993**, *98*, 5648−5652.
(18) (a) Schleyer, P. v. R.; Maerker, C.; Dransfeld, A.; Jiao, H.; Hommes, N. J. R. v. E. *J. Am. Chem. Soc.* **1996**, *118*, 6317−6318. (b) Subramanian, G.; Schleyer, P. v. R.; Jiao, H. *Organometallics* **1997**, *16*, 2362−2362.

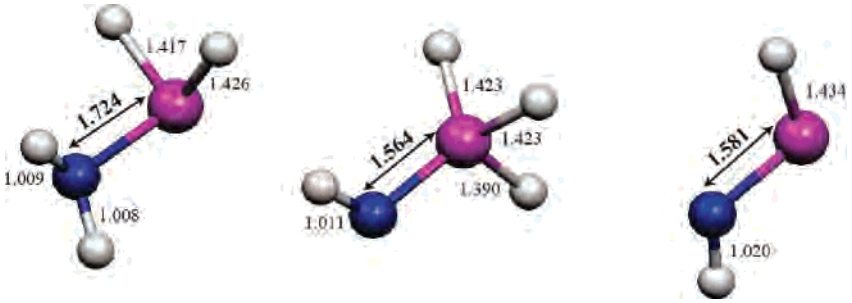

Figure 1. Optimized geometries of [H_2NPH_2], [$HNPH_3$], and [HNPH], showing bond lengths (Å).

Table 1. Important Geometrical Parameters[a]

	P−N (Å)	P−N−P (deg)	N−P−N (deg)	P−X (Å)	X−P−X (deg)	max dop[b] (Å)
[$N_3P_3H_6$]	1.606	121.3	118.7	1.406	101.0	0.000
[$N_3P_3F_6$]	1.576	120.8	119.2	1.551	98.2	0.000
(ref 29)	(1.570(6))	(121.0(4))	(119.0(2))	(1.526(4))	(98.6(8))	(0.014)
[$N_3P_3Cl_6$]	1.589	121.3	118.7	2.040	101.6	0.000
(ref 30)	(1.575(5))	(121.4(4))	(118.4(3))	(1.985(4))	(101.4(2))	(0.040)
[$N_3P_3Br_6$]	1.593	124.4	118.6	2.226	102.4	0.000
(ref 31)	(1.576(12))	(121(2))	(118.6(11))	(2.163(6))	(102.1(2))	(0.026)
[$N_3P_3(CH_3)_6$]	1.611	122.5	117.5	1.821	103.4	0.008
(ref 32)[c]	(1.61(2))	(124.0(6))	(114.7(9))	(1.789(11))	(105(2))	(0.085)
[$N_3P_3(CF_3)_6$]	1.593	120.1	119.8	1.887	103.9	0.000
(ref 29)	(1.581(5))	(120.2(4))	(119.8(3))	(1.852(15))	(102.9(5))	(0.018)
[$N_3P_3(NC_2H_4)_6$]	1.597, 1.610	123.2	116.7	1.688	98.9	0.011
(ref 33)	(1.5869(7), 1.6014(8))	(122.93(4))	(116.99(4))	(1.678(3))	(99.40(3))	(0.016)
[$N_3P_3(O_2C_6H_4)_3$]	1.585	122.2	117.8	1.631	95.9	0.001
(ref 34)	(1.56(2))	(123(2))	(116.5(10))	(1.605(9))	(96.7(9))	(0.049)
[$N_4P_4Cl_8$]	1.578	132.8	121.6	2.043	102.7	0.520
(ref 25a)	(1.570(9))	(131.3(6))	(121.2(5))	(1.989(6))	(102.8(2))	(0.474)
H[$NPCl_2$]$_4$H[d]	1.554, 1.615	131.4	113.6	2.064	100.8	0.001

[a] Values are averaged. Experimental quantities, with esds, are shown in parentheses. X refers to the substituent atom bound directly to P. [b] Maximum ring-atom distance out of the least-squares plane, defined by the ring atoms. [c] I_2 adduct. [d] Terminal NH and PCl_2H groups excluded from the average.

at the nonweighted mean of the ring atom coordinates using the GIAO method implemented in Gaussian98, both in the plane (NICS(0)) and 1 Å out of the plane (NICS(1)).

The natural bond orbital (NBO) analysis was carried out using the NBO 5.0 program,[19] ran through Gaussian98. For the natural chemical shielding analysis (NCS)[20] of the NICS ghost atoms, it was necessary in some cases to use smaller basis sets than those used for the geometry optimizations and frequency calculations because of memory limitations (see Supporting Information, section S4). NBO deletion analysis was carried out at the Hartree−Fock level on the optimized structures with the same basis sets, as density functional methods are often poorly parametrized for these calculations.[21]

The topological analysis of the B3LYP electron density was carried out using the AIMPAC suite of programs.[22] For [$N_3P_3Br_6$], [$N_3P_3(O_2C_6H_4)_3$], [$N_3P_3(NC_2H_4)_6$], and [$N_3P_3(CF_3)_6$] the 6-31G(d,p) basis set for all atoms was used to generate the AIMPAC input file. The average electron population, N(A) of an atom, A, was obtained by the integration of charge density over the basin of the atom, and its net charge, Q(A), was given by the difference between the nuclear charge and the electron population.

$$Q(\mathrm{A}) = Z_{\mathrm{A}} - N(\mathrm{A}) \tag{1}$$

The atomic localization index λ(A) represents the number of electrons localized in the basin of A. The delocalization index, δ(A,B), the number of electrons shared between the basins A and B, was calculated using eq 2.[23] S_{ij}(A) is the overlap integral between molecular orbitals i and j within the basin of A.

$$\delta(A,B) = 4\sum_{i,j}^{N/2} S_{ij}(\mathrm{A})S_{ij}(\mathrm{B}) \tag{2}$$

Illustrations were created using MOLEKEL.[24]

3. Results and Discussion

3.1. Phosphazene Geometry Optimizations. In addition to a range of cyclotriphosphazenes with different substituents, the puckered cyclotetraphosphazene, [$N_4P_4Cl_8$], and the model polyphosphazene, H[$NPCl_2$]$_4$H, have been investigated. In the former case, both "crown", C_{4v}, and "boat", D_{2d}, conformations have been characterized in the solid sate.[25] We attempted optimizations starting from both these conformations, although only the boat conformation was found to result in a minimum, consistent with both solution IR

(19) Glendening, E. D.; Badenhoop, J. K.; Reed, A. E.; Carpenter, J. E.; Bohmann, J. A.; Morales, C. M.; Weinhold, F. *NBO*, version 5.0; Theoretical Chemistry Institute, University of Wisconsin: Madison, WI, 2001.
(20) Bohmann, J. A.; Wienhold, F.; Farrar, T. C. *J. Chem. Phys.* **1997**, *107*, 1173−1184.
(21) Weinhold, F., Ed.; *NBO 5.0 Program Manual*; Theoretical Chemistry Institute, University of Wisconsin: Madison, WI, 2001.
(22) Biegler-Köning, F. W.; Bader, R. F. W.; Tang, T. H. *J. Comput. Chem.* **1982**, *3*, 317.
(23) Poater, J.; García-Cruz, I.; Illas, F.; Solà, M. *Phys. Chem. Chem. Phys.* **2004**, *6*, 314−318.
(24) Flükiger, P.; Lüthi, H. P.; Portmann, S.; Weber, J. *MOLEKEL*, version 4.0; Swiss Center for Scientific Computing: Manno, Switzerland, 2000.
(25) (a) Hazekamp, R.; Migchelson, T.; Vos, A. *Acta Crystallogr.* **1962**, *15*, 539−543. (b) Wagner, A. J.; Vos, A. *Acta Crystallogr.* **1968**, *B24*, 707−713.

Table 2. Bond Order and Delocalization Indices for a Series of Phosphazenes and Related Molecules[a]

	NLMO/NPA bond orders[b]						delocalization indices[c]			
	P−N	P−X	P−P	Σ_P	Σ_N	Σ_X	δ(P,N)	δ(P,X)	δ(N,N)	δ(N,X)
$[H_2NPH_2]$	0.61	0.92		2.44	1.80	0.89	0.88	0.87		0.12
$[HNPH_3]$	0.94	0.90[d]		3.72	1.41	0.76[d]	1.11	0.73[d]		0.15[d]
		0.94[e]				0.91[e]		0.73[e]		0.12[e]
[HNPH]	1.33	0.88		2.22	1.95	0.86	1.65	0.88		0.17
$[N_3P_3H_6]$	0.70	0.91	0.13	3.57	1.18	0.87	0.81	0.68	0.19	0.12
$[N_3P_3F_6]$	0.71	0.42	0.20	2.67	1.26	0.39	0.75	0.49	0.19	0.15
$[N_3P_3Cl_6]$	0.71	0.74	0.21	3.14	1.23	0.56	0.84	0.79	0.18	0.16
$[N_3P_3Br_6]$[f]	0.70	0.81	0.20	3.23	1.15	0.58	0.84	0.87	0.20	0.15
$[N_3P_3(CH_3)_6]$	0.68	0.72	0.14	3.18	1.14	2.97	0.80	0.73	0.18	0.11
$[N_3P_3(CF_3)_6]$[f]	0.71	0.68	0.17	3.12	1.19	2.50	0.76	0.55	0.20	0.10
$[N_3P_3(NC_2H_4)_6]$[f]	0.68[s]	0.52	0.15	2.75	1.08	2.04	0.68[s]	0.52	0.20	0.15[s]
	0.67[l]						0.68[l]			0.15[l]
$[N_3P_3(O_2C_6H_4)_3]$[f]	0.71	0.46	0.18	2.63	1.33	1.03	0.70	0.48	0.22	0.15
$[N_4P_4Cl_8]$	0.70	0.74	0.20[g]	3.09	1.16	0.59	0.84	0.78	0.17[g]	0.17
$H[NPCl_2]_4H$[h]	0.75[s]	0.71	0.12	2.91	1.15	0.52	0.92[s]	0.78	0.18	0.16[s]
	0.59[l]						0.75[l]			0.16[l]

[a] Values are averaged. X refers to the substituent atom bound directly to P. [b] The absolute bond order values for N−N and N−X bond orders for all molecules were ≤0.05. [c] The values of δ(P,P) for all molecules were ≤0.02. [d] H atoms syn to the N−H bond. [e] H atom anti to the N−H bond. [f] Using the 6-31G(d,p) basis set to generate the AIMPAC input file. [g] Not including cross ring P−P or N−N values. [h] Terminal NH and PCl_2H groups excluded from the average. [s] Quantity across the shorter P−N bond. [l] Quantity across the longer P−N bond.

spectra and previous ab initio calculations indicating that it is the lowest energy conformation.[3,11,26] The linear phosphazene oligomer, $H[NPCl_2]_4H$, was optimized starting from a planar *cis,trans*-conformation, which was retained and subsequently confirmed as a minimum by Hessian analysis. Hydride phosphazene derivatives are not known to exist, and the hypothetical phosphazene $[N_3P_3H_6]$ was only included as a useful theoretical reference.

The pertinent geometrical parameters of the optimized phosphazene geometries are given in Table 1. All of the cyclotriphosphazene derivatives have planar ring conformations and, with the exception of the $-NC_2H_4$ derivative, equal P−N bond lengths of ca. 1.59 Å. In general, both the P−N and P−R bond lengths are in good agreement with the known experimental values, and the computed bond length alternation found in the $-NC_2H_4$ derivative reproduces the experimental value well (0.013 vs 0.015(2) Å,[33] respectively). The bond length alternation is significantly larger in $H[NPCl_2]_4H$ (ca. 0.06 Å) in agreement with that previously calculated in *cis,trans*-$H[NPCl_2]_3H$ (ca. 0.06 Å)[14] and similar to those measured in the solid state for related oligomeric phosphazenes (ca. 0.07 Å),[27] although smaller than those reported for the solid-state structure of *cis,trans*-$[PNCl_2]_n$ (0.23(13) Å).[28]

The bond angles about the P and N centers in the phosphazenes are also well reproduced. Within the cyclotriphosphazenes, the P−N−P angles are slightly larger than the N−P−N angles (122(1) vs 118(1)°). In contrast, the P−N−P angles in $[N_4P_4Cl_8]$ (132.8°) and $H[NPCl_2]_4H$ (131.4°) are markedly widened in comparison to the N−P−N angles (121.6 and 113.6°, respectively), that are more like the cyclotriphosphazene values. These observations are in agreement with the general observation that the P−N−P angle is more flexible, ranging from 119 to 149°, than the N−P−N angle which is approximately 120° regardless of the ring size or chain length.[3] The force constant for the N−P−N bend in $ClNPCl_2NCl_2$ (N−P−N = 122.0°) has been calculated to be approximately 30 times that for the P−N−P bend in Cl_3PNPCl_4 (P−N−P = 173.8°), reinforcing this trend.[15]

3.2. Characterization of the P−N Bond. When attempting to characterize the phosphazene P−N bond, it is instructive to make a comparison to the hypothetical molecules, $[H_2NPH_2]$, $[HNPH_3]$, and [HNPH], which are depicted in Figure 1 in their lowest energy conformations. In the valence-bond picture, the P−N bond can be regarded as a double bond in [HNPH] and a single bond in $[H_2NPH_2]$, and the computed P−N bond lengths (1.581 and 1.724 Å), NLMO/NPA bond orders (1.33 and 0.61), and delocalization indices (1.65 and 0.88, respectively) are entirely consistent with this interpretation (see Table 2 and Supporting Information sections S2 and S3). In the case of the phosphazenes, while the bond lengths resemble that of the formal double bond in [HNPH], the corresponding NLMO/NPA bond orders, 0.70(3), and the delocalization indices, 0.79(7), are more like that of the formal single bond in $[H_2NPH_2]$. Similar observations hold for the model phosphazene, $[HNPH_3]$, although both the NLMO/NPA bond order, 0.94, and delocalization index, 1.11, are more intermediate. There is little variation in the P−N bond orders and delocalization indices in the cyclophosphazenes, although the observed bond-length alternation in $H[NPCl_2]_4H$ does result in significantly different bond orders, 0.75 and 0.59, and delocalization indices, 0.92 and 0.75 (values for the short and long P−N bonds, respectively). Only marginal differences (in the third decimal places) are observed for $[N_3P_3(NC_2H_4)_6]$, in which the alternation is much less in comparison.

(26) Breza, M. *Polyhedron* **2003**, *22*, 3243−3248.
(27) Allcock, H. R.; Tollefson, N. M.; Arcus, R. A.; Whittle, R. R. *J. Am. Chem. Soc.* **1985**, *107*, 5166−5177.
(28) Chatani, Y.; Yatsuyanagi, K. *Macromolecules* **1987**, *20*, 1042−1045.
(29) Singh, R. P.; Vij, A.; Kirchmeier, R. L.; Shreeve, J. M. *Inorg. Chem.* **2000**, *39*, 375−377.
(30) Bullen, G. J. *J. Chem. Soc. A* **1971**, 1450−1453.
(31) Zoer, H.; Wagner, A. J. *Acta Crystallogr.* **1970**, *B26*, 1812−1819.
(32) Markila, P. L.; Trotter, J. *Can. J. Chem.* **1974**, *52*, 2197−2200.
(33) Cameron, T. S.; Borecka, B.; Kwiatkowski, W. *J. Am. Chem. Soc.* **1994**, *116*, 1211−1219.

Table 3. Atomic Charges in a Series of Phosphazenes and Related Molecules[a]

	charge (NPA)[36]			atomic charge (and electron localization)[b]					
	P	N	X	*Q*(P)	*Q*(N)	*Q*(X)	λ(P)	λ(N)	λ(X)
$[H_2NPH_2]$	+0.53	−1.14	−0.07	+1.56	−1.31	−0.47	12.10	6.86	0.91
$[HNPH_3]$	+1.14	−1.28	−0.09[c]	+2.67	−1.60	−0.47[c]	10.67	7.39	0.94[c]
			−0.05[d]			−0.47[d]			0.95[d]
[HNPH]	+0.77	−1.01	−0.11	+1.47	−1.35	−0.45	12.25	7.00	0.91
$[N_3P_3H_6]$	+1.63	−1.46	−0.09	+2.98	−2.02	−0.48	10.47	7.77	0.96
$[N_3P_3F_6]$	+2.53	−1.47	−0.53	+3.54	−2.00	−0.77	10.18	7.74	9.27
$[N_3P_3Cl_6]$	+1.84	−1.45	−0.20	+2.82	−1.95	−0.44	10.50	7.60	16.77
$[N_3P_3Br_6]$[e]	+1.69	−1.46	−0.12	+2.54	−2.05	−0.25	10.70	7.70	34.55
$[N_3P_3(CH_3)_6]$	+2.01	−1.49	−1.06	+2.80	−2.04	−0.40	10.54	7.75	4.39
$[N_3P_3(CF_3)_6]$[e]	+1.80	−1.42	+0.81	+3.12	−2.08	+1.26	10.40	7.80	3.15
$[N_3P_3(NC_2H_4)_6]$[e]	+2.35	−1.49	−0.85	+3.51	−2.14	−1.35	10.21	7.82	6.72
$[N_3P_3(O_2C_6H_4)_3]$[e]	+2.44	−1.44	−0.77	+3.59	−2.11	−1.57	10.17	7.86	8.24
$[N_4P_4Cl_8]$	+1.88	−1.48	−0.20	+2.83	−1.97	−0.44	10.49	7.61	16.76
$H[NPCl_2]_4H$[f]	+1.86	−1.46	−0.23	+2.78	−1.95	−0.45	10.53	7.58	16.77

[a] Values are averaged. X refers to the substituent atom bound directly to P. [b] Determined by topological analysis of the electron density. [c] H atoms syn to the N−H bond. [d] H atom anti to the N−H bond. [e] Using the 6-31G(d,p) basis set to generate the AIMPAC input file. [f] Terminal NH and PCl_2H groups excluded from the average.

In the zwitterionic model, one electron is formally transferred from P to N, in accordance with their electronegativity difference. Calculated atomic charges are certainly consistent with this interpretation (Table 3). The hypothetical molecules, [HNPH], $[HNPH_3]$, and $[H_2NPH_2]$, are again useful for illustrating this proposal. In both [HNPH] and $[H_2NPH_2]$, the P and N atomic charges are similar, whereas in $[HNPH_3]$ they are significantly larger in magnitude. The charge separation between P and N is larger again in the phosphazenes, primarily because of the larger charge on the P center. The value of this charge separation varies significantly depending on (the electron-withdrawing capacity of) the substituent and is particularly pronounced in the −F, $-CF_3$, and $-NC_2H_4$ derivatives. An approximate inverse correlation between the P/N charge difference and the P−N bond length exists. Also, the large variations in the P−N−P angle found in phosphazenes could be attributed to the substituent-dependent charge at the P centers. For example, the observed bond angles in solid-state structures of *boat*-$[N_4P_4F_8]$ (P−N−P, 140.4°; N−P−N, 123.1°) and *boat*-$[N_4P_4Cl_8]$ (P−N−P, 131.4°; N−P−N = 121.2°) are consistent with this argument.[25a,35]

A recent topological analysis of a series of cyclotriphosphazenes by Luaña and co-workers is also consistent with this perspective,[15] where the phosphazene bond consists of one highly polarized σ bond contracted by electrostatic interactions. This analysis, confirmed by our similar analysis (using instead density functional theory and larger basis sets, see Supporting Information section S2) of the molecules in this investigation, indicates a significant degree of charge transfer from the P centers to those of N and the substituents, as demonstrated by low P-electron localization values, λ, and corresponding enlarged *N* values and, to a lesser extent, *X* values (Table 3). There is, however, a considerable degree of delocalization between the centers, as revealed by the calculated delocalization values (Table 2). The Laplacian of the electron density, $\nabla^2\rho$, which measures whether the electron density is locally concentrated ($\nabla^2\rho < 0$) or depleted ($\nabla^2\rho > 0$), at the P−N bond critical points are, in all cases, noticeably positive, indicating that these bonds have predominately ionic character (see Table S-3). In contrast, the Laplacian for the majority of the P−X bonds is negative, indicating increased covalency. For the highly electron-withdrawing substituents, −F, $-NC_3H_4$, and $-O_2C_6H_4$, positive values are observed, consistent with the large degree of P/X charge separation in these derivatives.

3.3. Natural Bond Orbital Analysis. To further investigate the electronic structure of the phosphazenes, we carried out a natural bond orbital (NBO) analysis. In this scheme, the molecular-wave function is represented as an orthonormal set of Lewis-type lone pair and bonding orbitals, with small corrections being made via occupancy of non-Lewis-type antibonding and Rydberg orbitals.[37] With this in mind and on the basis of preceding P−N bond characterization, the zwitterionic phosphazene model was chosen as the parent Lewis structure for the NBO analysis via the NBO $CHOOSE keyword.[38] In doing so, inspection of the occupancy of the corresponding non-Lewis-type NBOs allows the assessment of this model's validity in representing the electronic structure of phosphazenes. Moreover, departures from the idealized Lewis structure and delocalization can be analyzed by the interactions of the non-Lewis-type NBOs.

Phosphazene NBO occupancies, using the zwitterionic model as a parent Lewis structure, are listed in Table 4. The total non-Lewis populations are indicative of the significant occupation of antibonding-type NBOs (valence non-Lewis occupancy), indicative of the presence of delocalization. For comparison, alternative Lewis representations of $[N_3P_3Cl_6]$

(34) Allcock, H. R.; Levin, M. L.; Whittle, R. R. *Inorg. Chem.* **1986**, *25*, 41−47.
(35) Elias, A. J.; Twamley, B.; Haist, R.; Oberhammer, H.; Henkel, G.; Krebs, B.; Lork, E.; Mews, M.; Shreeve, J. M. *J. Am. Chem. Soc.* **2001**, *123*, 10299−10303.
(36) (a) Reed, A. E.; Weinhold, F. *J. Chem. Phys.* **1983**, *78*, 4066−4073. (b) Reed, A. E.; Weinstock, R. B.; Weinhold, F. *J. Chem. Phys.* **1985**, *83*, 735−746.
(37) (a) Foster, J. P.; Weinhold, F. *J. Am. Chem. Soc.* **1980**, *102*, 7211−7218. (b) Weinhold, F. *Encyclopedia of Computational Chemistry*; Schleyer, P. v. R., Allinger, N. L., Clark, T., Gasteiger, J., Kollman, O. A., Schaefer, H. F., III, Schreiner, P. R., Eds.; John Wiley & Sons: Chichester, U.K., 1998; Vol. 3, pp 1792−1811.
(38) NBO calculations were carried out using the NBO 5.0 program ran through Gaussian98.[16,21]

Table 4. Zwitterionic Model NBO Occupancies[a]

	total non-Lewis	valence non-Lewis	σ_{PN}	σ_{PX}	N_{lp1}	N_{lp2}	σ^*_{PN}	σ^*_{PX}	N(3,−3)[b] ρ/eÅ^{-3}
$[N_3P_3H_6]$	1.63	1.37	1.99	1.96	1.79	1.76	0.10	0.12	0.480
$[N_3P_3F_6]$	2.46	1.95	1.98	1.98	1.77	1.71	0.14	0.19	0.488
$[N_3P_3Cl_6]$	2.74	2.16	1.98	1.96	1.78	1.69	0.16	0.20	0.494
$[N_3P_3Br_6]$	2.81	2.26	1.98	1.95	1.79	1.68	0.17	0.21	0.505
$[N_3P_3(CH_3)_6]$	1.76	1.42	1.99	1.98	1.80	1.77	0.10	0.12	0.480
$[P_3N_3(CF_3)_6]$	4.46	3.64	1.99	1.96	1.77	1.73	0.11	0.20	0.495
$[N_3P_3(NC_2H_4)_6]$	3.17	2.57	1.98[d] 1.98[e]	1.97	1.81	1.73	0.11[d] 0.15[e]	0.16	0.497
$[N_3P_3(O_2C_6H_4)_3]$	6.85	6.17	1.98	1.99	1.79	1.70	0.14	0.18	0.503
$[N_4P_4Cl_8]$	3.54	2.79	1.98	1.96	1.78	1.72	0.16	0.19	0.490
$H[NPCl_2]_4H$	3.68	2.94	1.98[c,d] 1.97[c,e]	1.96[c]	1.78[c]	1.71[c]	0.13[c,d] 0.14[c,e]	0.24[c]	0.487[c]

[a] Values are averaged. X refers to the substituent atom bound directly to P. lp1 is the lone-pair NBO in the plane; lp2 is the corresponding NBO perpendicular to the plane. [b] Localized concentrations of electron density [(3, −3) critical points] found ca. 0.4 Å from the N centers. [c] Terminal NH and PCl_2H groups excluded from the average. [d] Quantity across the shorter P−N bond. [e] Quantity across the longer P−N bond.

were assessed. Both models with alternating double−single P−N bonds in-plane (via the $CHOOSE keyword[38]) and out-of-plane (default NBO algorithm[38]) have larger total non-Lewis occupancies, 3.11 and 2.97, respectively, and the corresponding double-bond P−N NBOs are highly skewed toward nitrogen, 95.5% and 92.2%, respectively, essentially corresponding to lone pair N_p NBOs. In this respect, the most tractable reference Lewis model is confirmed to be the zwitterionic one.

The magnitudes of both the σ^*_{PN} and σ^*_{PX} NBO occupancies indicate that the primary correction necessary for agreement with the molecular-wave function is delocalization into these NBOs, and together, they account for almost all of the valence non-Lewis population. For the $-O_2C_6H_4$, $-NC_2H_4$, and $-CF_3$ derivatives, the additional delocalization is substituent localized, typified in the $-O_2C_6H_4$ derivate where these corrections are necessary for an accurate representation of aromatic resonance in the benzene moiety. The source of this delocalization is identified by the low N lone-pair NBO populations which deviate significantly from their ideal occupancy of 2.0 e^-, consistent with the noticeable δ(N,X) values, validating the presence of negative hyperconjugation. The low P_{3d} occupancies (<0.13 e^- per P atom) found in the NPA analysis are not indicative of valence d-orbital predication but are necessary for the description of P−N and particularly the P−X bonds: ca. 1% and 2% of the total d orbital contributions to the $\sigma_{PN}/\sigma^*_{PN}$ and $\sigma_{PX}/\sigma^*_{PX}$ NBOs in the zwitterionic model, respectively.

The occupancies of the σ^*_{PN} and σ^*_{PX} NBOs account for ca. 15% of the P and N valence electrons not involved in σ bonding, indicating the ionic representation as the dominant underlying feature in the electronic structure of these compounds. The conclusion for a natural resonance theory (NRT)[39] analysis of the model compound, $[H_2NPH_2]$, is similar (see Supporting Information section S3). In this scheme, the zwitterionic model is found to be the dominant resonance form for explaining the bonding (79.2% weight). Multiple-bond character via negative hyperconjugation is found to be necessary for a more complete representation with two dominant forms (each 7.8% weighting) corresponding to complete negative hyperconjugation from a N_{lp} NBO to either of the *syn*-σ^*_{PH} (to the N−H bond) NBOs (Figure 2). For comparison, the dominant resonance structures of $[H_2NPH_2]$ and [HNPH] involve formal P−N single and double bonds, with weightings of 94.8% and 97.2%, respectively. Although such an analysis of the phosphazenes was not possible, from the magnitudes of the σ^*_{PN} and σ^*_{PX} NBO occupancies, we conclude that negative hyperconjugation is a necessary modification to the largely highly polarized σ bonding in the phosphazenes as explicitly expressed by the result of the NRT analysis of $[HNPH_3]$.

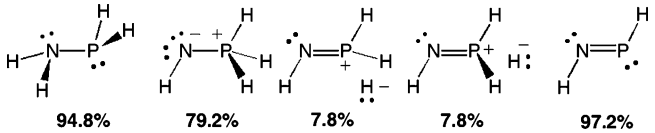

Figure 2. Dominant contributing resonance structures of $[H_2NPH_2]$, $[HNPH_3]$, and [HNPH].

In accordance with the large charge separation between P and N, the σ_{PN} NBOs are localized on N, though to a similar extent for all the phosphazenes, ca. 72%. Although not to the same degree, the σ_{PX} NBOs are also polarized, with the corresponding X localization ranging from 51.8% for the −H derivative to 81.4% for the −F derivative. These values can largely be correlated with the corresponding N and X atomic charges, see Table 3. In contrast, the relative charge invariance on N is reflected in the similarity of the σ_{PN} NBO localizations. The extent of negative hyperconjugation, as indicated by occupation of the σ^*_{PN} and σ^*_{PX} NBOs and low occupancies of the N_{lp1} and N_{lp2} NBOs, varies significantly with the nature of the substituent. Variations in the magnitude of lone pair-like concentrations [(3, −3) critical points] of electron density near N centers, identified in the topological analysis (see Table 4 and Supporting Information section S2), also show similar variations with substituent. These variations, particularly in the occupancies of the N_{lp1} and N_{lp2} NBOs and the ρ at the N (3, −3), cannot be explained by the atomic charges alone, as notably the N NPA and atomic charges are practically the same for all of the phosphazenes. To rationalize these variations, the Lewis-type donor and non-Lewis-type acceptor NBO interactions,

(39) (a) Glendening, E. D.; Weinhold, F. *J. Comput. Chem.* **1998**, *19*, 592. (b) Glendening, E. D.; Weinhold, F. *J. Comput. Chem.* **1998**, *19*, 610. (c) Glendening, E. D.; Badenhoop, J. K.; Weinhold, F. *J. Comput. Chem.* **1998**, *16*, 628.

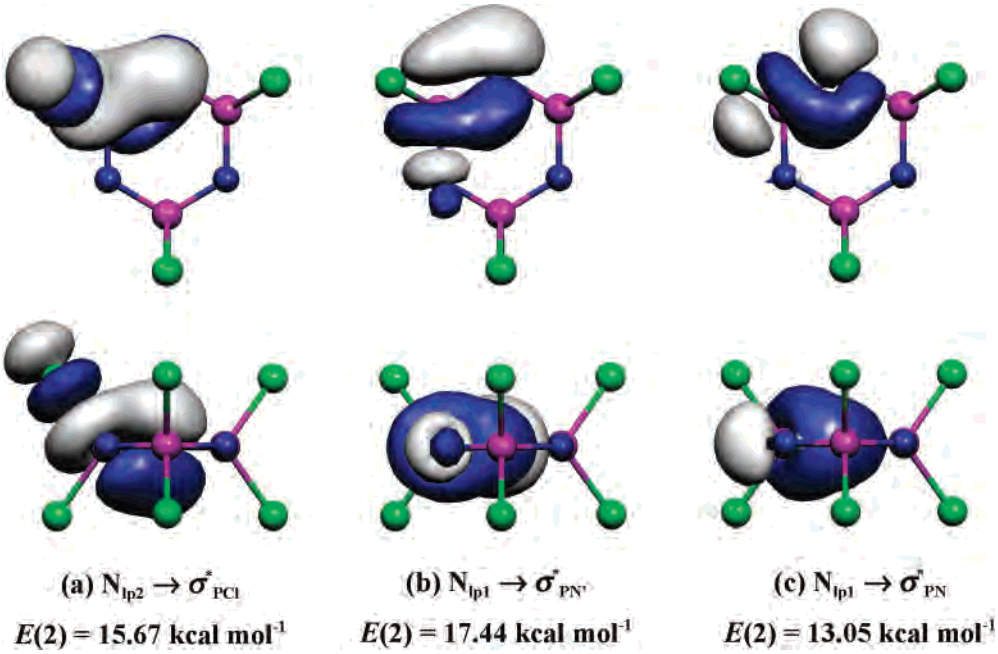

Figure 3. Major NBO overlaps in $[N_3P_3Cl_6]$: (a) $N_{lp2} \rightarrow \sigma^*_{PCl}$, (b) $N_{lp1} \rightarrow \sigma^*_{PN'}$, and (c) $N_{lp1} \rightarrow \sigma^*_{PN}$.

Table 5. Energetic Analysis of NBO Donor−Acceptor Interactions[a]

	deletion analysis, ΔE_{SCF} (kcal mol^{-1})				perturbation analysis, $E(2)$ (kcal mol^{-1})			
	Del *[b]	Del σ^*_{PN+PX}	Del σ^*_{PN}	Del σ^*_{PX}	$N_{lp2} \rightarrow \sigma^*_{PX}$	$N_{lp1} \rightarrow \sigma^*_{PN'}$	$N_{lp1} \rightarrow \sigma^*_{PN}$	other[c]
$[N_3P_3H_6]$	776	493	244	231	10.81	16.18	12.16	
$[N_3P_3F_6]$	1272	873	365	456	15.40	15.23	15.72	$F_{lp} \rightarrow \sigma^*_{PF}$, ca. 12
$[N_3P_3Cl_6]$	1168	763	385	349	15.67	17.44	13.05	
$[N_3P_3Br_6]$	1129	738	372	332	16.59	17.60	12.47	
$[N_3P_3(CH_3)_6]$	862	512	263	231	10.70	16.54	10.74	
$[N_3P_3(CF_3)_6]$	2137	731	289	413	13.53	16.24	13.35	$F_{lp} \rightarrow \sigma^*_{CF}$, ca. 12
$[N_3P_3(NC_2H_4)_6]$	1760	716	315	376	12.41[f]	16.92[f]	8.10[f]	$X_{lp} \rightarrow \sigma^*_{PN}$[d], ca. 8
			140[f]		12.93[g]	15.15[f]	11.14[g]	
			182[g]					
$[N_3P_3(O_2C_6H_4)_3]$	2660	783	330	420	14.79	15.34	11.87	$\pi_{CC} \rightarrow \pi^*_{CC}$, ca. 22 $O_{lp} \rightarrow \pi^*_{CC}$, ca. 21
$[N_4P_4Cl_8]$	1500	988	502	382	23.65 5.53	17.09	5.39	$N_{lp1} \rightarrow \sigma^*_{PCl}$, ca. 6
$H[NPCl_2]H$	1522	988	453	512				
			238[f]					
			218[g]					
		796[e]	272[e]	403[e]	19.97[e,f]	9.83[e,f]	3.68[e,f]	$N_{lp1} \rightarrow \sigma^*_{PCl}$, ca. 9[e,f]
			107[e,f]		12.79[e,g]	12.15[e,g]	4.30[e,g]	
			165[e,g]					

[a] Values are averaged. X refers to the substituent atom bound directly to P. lp1 is the lone-pair NBO in the plane; lp2 is the corresponding NBO perpendicular to the plane. [b] Deletion of all non-Lewis NBOs. [c] Other interactions with significant $E(2)$ values. [d] Long P−N bond. [e] Terminal NH and PCl_2H groups excluded from the average. [f] Quantity across the shorter P−N bond. [g] Quantity across the longer P−N bond.

responsible for these delocalizations, were investigated. An intuitive measure of the effectiveness of these interactions can be estimated by second-order perturbation theory according to eq 3.

$$E(2) = \frac{q_i[F(i,j)]^2}{\epsilon_i - \epsilon_j} \tag{3}$$

This equation evaluates the magnitude of the donor−acceptor interaction in terms of the spatial overlap of the NBOs, using the off-diagonal Fock-matrix elements $F(i,j)$, and the difference in energy between the NBOs, $\epsilon_i - \epsilon_j$, weighted by the occupancy of the donor NBO, q_i. Likewise, the energetic importance of these interactions can be assessed by NBO energetic analysis ($DEL orbital deletions[38]), where NBOs (alone or in combinations) are deleted and the approximate SCF energy recalculated. The major donor−acceptor interactions are illustrated in Figure 3 for $[N_3P_3Cl_6]$, with the corresponding energetic analysis summarized in Table 5.

Generalizing for the cyclotriphosphazenes, there are three dominant NBO interactions identified by large donor−acceptor $E(2)$ values in the perturbation analysis, see Figure 3. The spatial overlap is particularly good for the largest interaction, the in-plane $N_{lp1} \rightarrow \sigma^*_{PN}$ interaction, Figure 3b, because of the large P character of the σ^*_{PN} NBOs (ca. 72%), a direct consequence, once again, of the large charge separation between P and N. In the case of the −F derivative,

the large overlap for this interaction is offset by a larger than usual energy difference between the donor and acceptor NBOs, resulting in a lower $E(2)$ value than expected. The next most significant interaction is the out-of-plane $N_{lp2} \rightarrow \sigma^*_{PX}$ interaction, Figure 3a, with the associated $E(2)$ value encapsulating the combined effects of the substituents (see below). The remaining interaction, $N_{lp1} \rightarrow \sigma^*_{PN}$, shown in Figure 3c, is of relatively less importance in comparison, and the moderate spatial overlap is sensitive to the P−N−P angle. For example, in $[N_4P_4Cl_8]$ and $H[NPCl_2]_4H$, with much larger P−N−P angles, the $E(2)$ value for this interaction is reduced from ca. 12 kcal mol^{-1} in the cyclotriphosphazenes to 3−5 kcal mol^{-1}. In the halogen derivatives, the presence of suitably oriented substituent lone pair NBO results in $X_{lp} \rightarrow \sigma^*_{PX'}$ interactions, although with the exception of the −F derivative ($E(2)$ ca. 12 kcal mol^{-1}), these are generally weak ($E(2) < 8$ kcal mol^{-1}), and in all of these derivatives the lone pair NBOs have occupancies >1.94 e$^-$. Notably, the X_{lp} NBOs in the $-N(C_2H_4)$ derivative are not suitably oriented for such an interaction, and correspondingly, no significant negative hyperconjugation occurs across the exocyclic P−N bond.

For the cyclotriphosphazenes, the perturbation analysis can be used to explain the variations in the σ^*_{PN} and σ^*_{PX} NBO occupancies, with a high occupancy correlating with a stronger NBO interaction. In particular, the particularly low occupancies of the σ^*_{PX} NBOs in the −H and $-CH_3$ derivatives can be attributed to the weak interaction with the N_{lp2} NBOs (10.81 and 10.70 kcal mol^{-1}, respectively) because of the less polar character of the P−X bonds (P localization 51.8% and 62.1%, respectively). Likewise, the −F, −Cl, −Br, $-O_2C_6H_4$, and $-CF_3$ derivatives, with large σ^*_{PX} NBO occupancies, can be attributed to particularly good interactions as indicated by large $E(2)$ values ranging from 13.53 kcal mol^{-1} for $-CF_3$ to 16.59 kcal mol^{-1} for −Br.

The large deletion values found for the negative hyperconjugative interactions also reaffirm their importance in the bonding scheme, see Table 5. In each case, the principle effect of the σ^*_{PN} and σ^*_{PX} NBO deletions is the increased occupancy of N_{lp1} and N_{lp2} NBOs, respectively. While there is some variation among the σ^*_{PN} and σ^*_{PX} values, a clear correlation between the destabilization energy associated with the combined σ^*_{PN+PX} NBO deletion and the P−N bond lengths is observed (Figure 4).

The longer bond lengths in the $-NC_2H_4$ derivative do not fit well into this trend, deviating significantly above the least-squares regression line formed from the data of the other derivatives. Furthermore, in contrast with the trend, the destabilization energy of the corresponding $\sigma^*_{PN\ (long)}$ NBO is significantly larger than that of the $\sigma^*_{PN\ (short)}$ NBO. The origin of this apparent inconsistency is explained by the existence of an interaction between the nitrogen lone-pair NBO of the substituent (X_{lp}) and the $\sigma^*_{PN\ (long)}$ NBO ($E(2)$ ca. 8 kcal mol^{-1}) (Figure 5). This symmetry reinforced interaction results in the enhancement of the multiple-bond character for the shorter P−N bonds, increasing the σ^*_{PN} NBO occupancies of the longer P−N bonds (cf. 0.15, $\sigma^*_{PN\ (long)}$; 0.11, $\sigma^*_{PN\ (long)}$) by depletion of the X_{lp} NBO occupancy

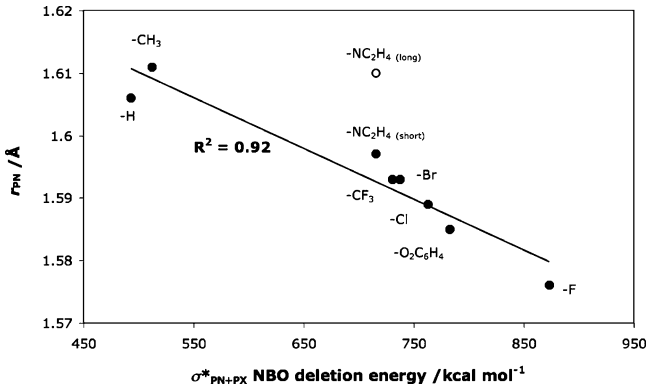

Figure 4. Calculated P−N bond length versus σ^*_{PN+PX} NBO deletion energy. The linear regression line ($R^2 = 0.92$) excludes the nonfilled data point $-NC_2H_{4\ (long)}$.

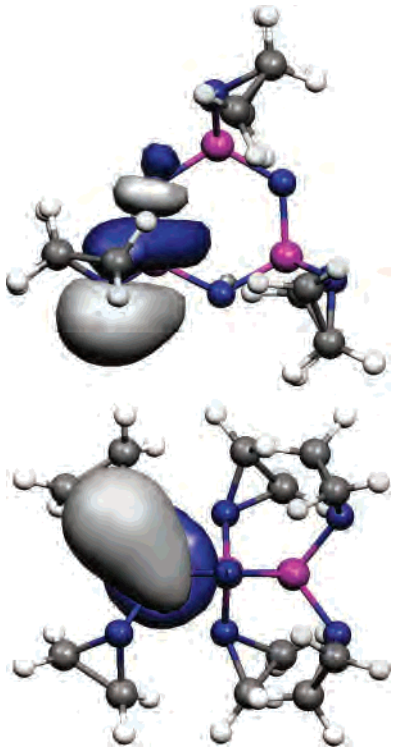

Figure 5. Selected NBO overlap in $[N_3P_3(NC_2H_4)_6]$: $X_{lp} \rightarrow \sigma^*_{PN\ (long)}$ ($E(2) \approx 8$ kcal mol^{-1}).

(1.91 e$^-$) and ultimately the observed bond length alternation found in this derivative. In the other derivates bearing substituent lone-pair NBOs, analogus interactions can be detected, but in each case, they are symmetrical and weaker.

Because of the lower symmetry of the cyclotetraphosphazene (D_{2d}), in comparison to that of the cyclotriphosphazenes (D_{3h}), there are two different types of $N_{lp2} \rightarrow \sigma^*_{PCl}$ NBO overlap, as depicted in Figure 6. The most effective of these two, Figure 6a, $E(2) = 23.65$ kcal mol^{-1} results from the spatial overlap of near parallel N_{lp2} and σ^*_{PCl} NBOs, whereas for the other, Figure 6b, $E(2) = 5.53$ kcal mol^{-1}, the corresponding NBOs are almost perpendicular. Both of these negative hyperconjugative interactions are balanced equally between the symmetry nonequivalent nitrogen atoms, the net result is equal occupation of the σ^*_{PCl} bonds (comparable in magnitude to those calculated for $[N_3P_3Cl_6]$) and correspondingly equal P−N bond lengths. Indeed, in

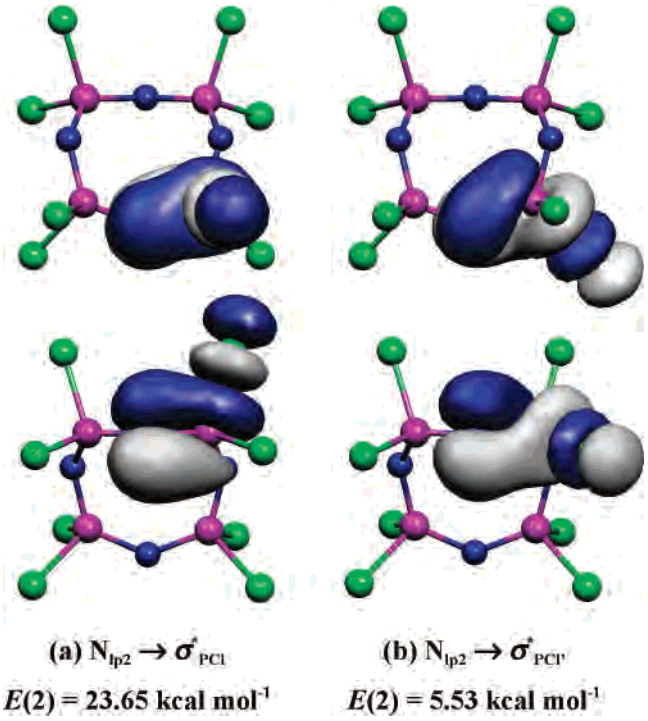

Figure 6. $N_{lp2} \rightarrow \sigma^*_{PCl}$ NBO overlaps in $[N_4P_4Cl_8]$: (a) $N_{lp2} \rightarrow \sigma^*_{PCl}$ and (b) $N_{lp2} \rightarrow \sigma^*_{PCl'}$.

many respects the P−N bonding characteristics in both $[N_3P_3Cl_6]$ and $[N_4P_4Cl_8]$ are the same: P−N NLMO/NPA bond orders (0.71 vs 0.70), delocalization indices (both 0.84), atomic and NPA charges (Table 3), ρ at the N (3, −3) (Table 4), and NBO occupancies (Table 4). Sun's conclusion that the phosphazene P−N bond has a low barrier of rotation, based on the comparison with those in $[H_2NPH_2]$ (6 kcal mol^{-1}), $[HNPH_3]$ (2 kcal mol^{-1}), and [NHPH] (44 kcal mol^{-1}),[14] is consistent with a dominant ionic-bonding component. Both P−N bonds in $[N_3P_3Cl_6]$ and $[N_4P_4Cl_8]$ have significant negative hyperconjugation contributions despite their differences in geometry, suggesting that the donor−acceptor interactions have a flexible character to them. To supplement Sun's calculations and test this hypothesis, the relaxed potential-energy surface for the P−N

Chart 2

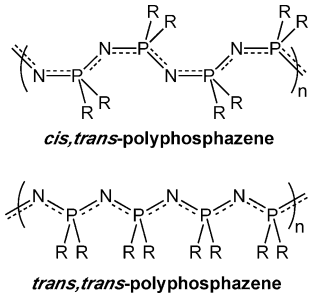

bond rotation in the hypothetical molecule $[HNPCl_3]$ has been computed as shown in Figure 7, and the effect on the occupancies of the N_{lp1} and N_{lp2} NBOs has been examined. The calculated rotation barrier of 1.4 kcal mol^{-1} is similar to that calculated for $[HNPH_3]$. Both values are much lower than that of the formal double P−N bond in [NHPH], and even that of the formal single bond in $[H_2NPH_2]$. The sum of the nitrogen lone-pair NBO occupancies, encapsulating the amount of negative hyperconjugation present, changes very little during the rotation (3.334 to 3.347 e$^-$), particularly over small deviations from the lowest-energy confirmation (ca. −15 to +15°). These observations reflect that on rotating the P−N bond from the energy minimum, reductions of the $N_{lp2} \rightarrow \sigma^*_{PCl2}$ and $\sigma^*_{PCl2'}$ NBO interactions are compensated by increased contributions from the $N_{lp2} \rightarrow \sigma^*_{PCl1}$ NBO interaction, as the spatial overlaps of the corresponding NBOs change (similarly for N_{lp1} interactions, labels as depicted in Figure 7). With this rationale, it appears that the contributions from the negative hyperconjugation build multiple-bond character into the P−N bond with minimal hindrance to bond rotation.

The phenomenon of P−N bond length alternation, generally confined to polyphosphazenes, is one of the most intriguing peculiarities of the phosphazene bond. The dominant conformational form adopted in these polymers is considered to be the *cis,trans*-conformation (or slight distortions thereof, see Chart 2).[2a,3,28] This conformation, presumably preferred by minimization of intramolecular steric repulsions, has previously been found to be more stable than

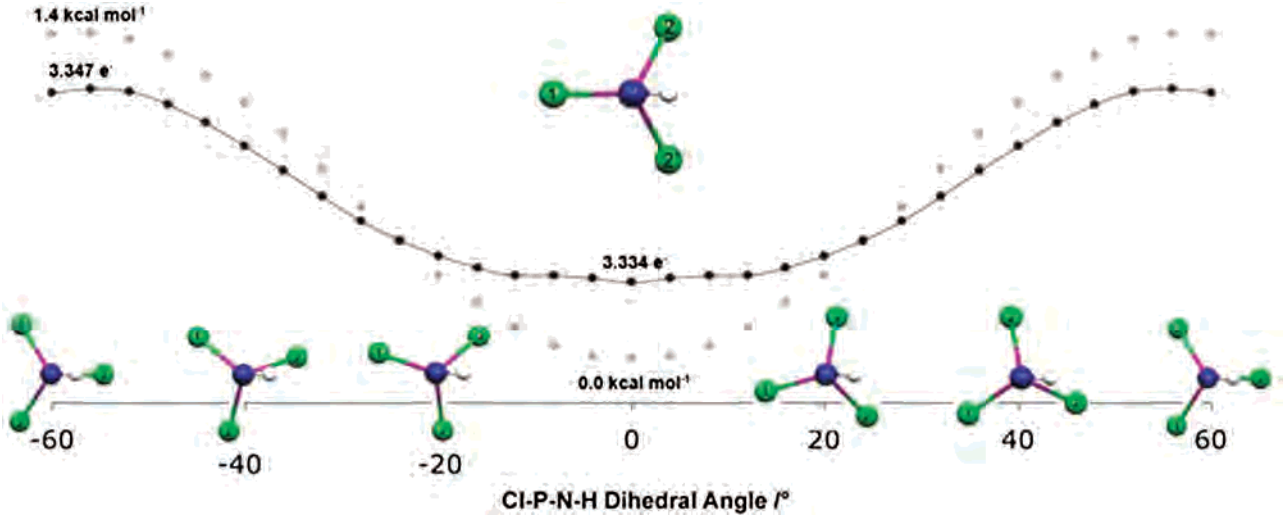

Figure 7. Relaxed potential-energy surface of $[HNPCl_3]$, energy is plotted in gray, and the combined $N_{lp1} + N_{lp2}$ NBO occupancies are plotted in black.

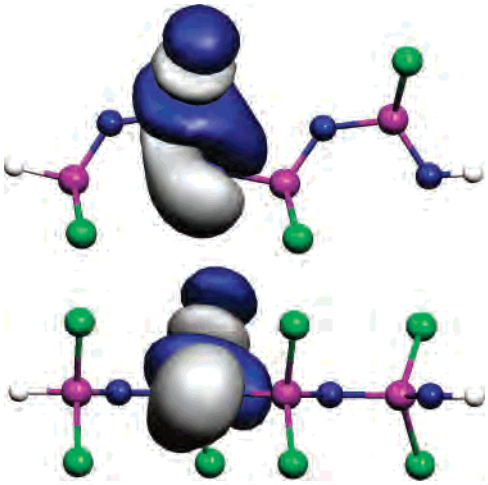

Figure 8. Selected NBO overlap in $H[NPCl_2]_4H$: $N_{lp1} \rightarrow cis\text{-}\sigma^*_{PCl}$ ($E(2) \approx 9$ kcal mol^{-1}).

a range of other alternative conformations, including the planar *trans,trans*-conformation, for a range of derivatives by both classical potential-energy calculations, using modified Lennard-Jones potentials,[40] and semiempirical CNDO/2 and MNDO methods.[41] These findings are further supported by the synthesis and characterization of short-chain phosphazene oligomers which are found to prefer the planar *cis,-trans*-conformation and which exhibt P−N bond length alternation.[27] Distortions from the planar *cis,trans*-conformation are, however, not unlikely because of the low rotation barriers, as described above.

In $H[NPCl_2]_4H$, the consequence of the *cis,trans*-conformation and the widened P−N−P bond angle is primarily the enhancement of the spatial overlap between N_{lp1} and the *cis*-σ^*_{PCl} NBOs (Figure 8), which are approximately three times larger than those of the corresponding trans interactions. This enforced spatial asymmetry leads to considerable differences in the extent of negative hyperconjugation across the different P−N bonds as indicated by their respective $E(2)$ values (cis, ca. 9.3; trans, ca. 1.2 kcal mol^{-1}). Those of the trans interactions are much the same as those found in the cyclotriphosphazenes (e.g., $E(2) = 1.7$ kcal mol^{-1} in the −Cl derivative). This difference offers a compelling explanation for the observed bond length alternation, providing a rationalization for the enhanced bond order in this oligomer and, by inference, related oligomeric species and polymeric polyphosphazenes in similar conformations. In comparison, there is also an enhanced $N_{lp1} \rightarrow \sigma^*_{PCl}$ interaction ($E(2) =$ 9.3 kcal mol^{-1}) in the cyclotetraphosphazene because of the conformational changes and an increased P−N−P angle; however, in this case, the interactions are symmetrical about the N centers. Similarly, symmetrical interactions would also be expected in polyphosphazenes in the planar *trans,trans*-conformation, in agreement with the absence of bond length alternation predicted for this conformer.[41a] Furthermore, in $H[NPCl_2]_4H$, across the shorter P−N bond, the $N_{lp2} \rightarrow \sigma^*_{PCl}$ NBO interaction is also stronger because of the closer proximity of NBOs, increasing the spatial overlap, although enhancement of the $N_{lp1} \rightarrow \sigma^*_{PN'}$ interaction across the longer P−N bond partially counteracts the factors that lead to the bond length alternation.

3.4. Extent of Delocalization. The electronic structure of inorganic benzene analogues continues to be of interest.[42] However, perhaps attributable to the difficulty in describing the bonding, cyclotriphosphazenes have often been overlooked as potential candidates, even though aromatic systems containing hypervalent centers are well-known.[43] While the cyclotriphosphazenes are generally characterized by planar ring structures with equal bond lengths, the presence of the primary electronic criteria of cyclic delocalization has remained uncertain. In an attempt to evaluate the presence of this delocalization, the commonly used nucleus independent chemical shift parameters (NICS(0) and NICS(1)), which attempt to quantify ring currents induced by cyclic delocalization, have been calculated.[18] In addition, para-delocalization indices (PDIs), defined as the mean delocalization index of para-related atoms in a six-membered ring, have also been determined.[44]

Table 6 contains the NICS and PDI values for phosphazenes and, for comparison purposes, benzene, $[B_3N_3H_6]$, and $[B_3P_3H_6]$. Aromatic rings, cf. benzene, are characterized by negative NICS values and nonaromatic compounds by positive values. NICS values calculated using the recommended 6-31+G(d) basis set are included for ease of comparison with literature data,[18a] as NICS quantities are known to be both ring-size and basis-set dependent.[18a,45] In comparison to benzene, only the phosphazenes with the most electron-withdrawing substituents (−F, −Cl, $-NC_2H_4$, $-O_2C_6H_4$) have NICS values that are suggestive of aromatic character (if only partial). The low NICS(0) value for hypothetical $[N_3P_3H_6]$ is in agreement with the previously calculated value (−1.2 vs −2.2) determined using a similar basis set.[42g] Together with the low delocalization in this derivative (valence non-Lewis population of 1.37 e$^-$), these data indicate that this molecule is a poor phosphazene model. For the cyclotriphosphazenes with the most electron-withdrawing substituents, these NICS values would place cyclotriphosphazenes among some of the most common inorganic benzene candidates, such as $[B_3N_3H_6]$ (nonaro-

(40) Allen, R. W.; Allcock, H. R. *Macromolecules* **1976**, *9*, 956−960.
(41) (a) Breza, M. *Eur. Polym. J.* **1999**, *35*, 581−586. (b) Tanaka, K.; Yamashita, S.; Yamabe, T. *Macromolecules* **1986**, *19*, 2062−2064.
(42) For recent examples, see: (a) Engelberts, J. J.; Havenith, R. W. A.; van Lenthe, J. H.; Jenneskens, L. W.; Fowler, P. W. *Inorg. Chem.* **2005**, *44*, 5266−5272. (b) Soncini, A.; Domene, C.; Engelberts, J. J.; Fowler, P. W.; Rassat, A.; van Lenthe, J. H.; Havenith, R. W. A.; Jenneskens, L. W. *Chem.—Eur. J.* **2005**, *11*, 1257−1266. (c) Li, Z.-H.; Moran, D.; Fan, K.-N.; Schleyer, P. c. R. *J. Phys. Chem. A* **2005**, *109*, 3711−3716. (d) Proft, F. D.; Fowler, P. W.; Havenith, R. W. A.; Schleyer, P. v. R.; Lier, G. C.; Geerlings, P. *Chem.—Eur. J.* **2004**, *10*, 940−950. (e) Fowler, P. W.; Rees, C. W.; Soncini, A. *J. Am. Chem. Soc.* **2004**, *126*, 11202−11212. (f) Boughdiri, S.; Hussein, K.; Tangour, B.; Dahrouch, M.; Rivière-Baudet, M.; Barthelat, J.-C. *J. Organomet. Chem.* **2004**, *689*, 3279−3286. (g) Jemmis, E. D.; Kiran, B. *Inorg. Chem.* **1998**, *37*, 2110−2116. (h) Schleyer, P. v. R.; Jiao, H.; Hommes, N. J. R. v. E.; Malkin, V. G.; Malkina, O. L. *J. Am. Chem. Soc.* **1997**, *119*, 12669−12670.
(43) Minkin V. I.; Minyaev, R. M. *Chem. Rev.* **2001**, *101*, 1247−1265.
(44) (a) Poater, J.; Fradera, X.; Duran, M.; Solà, M. *Chem.—Eur. J.* **2003**, *9*, 400−406. (b) Poater, J.; Fradera, X.; Duran, M.; Solà, M. *Chem.—Eur. J.* **2003**, *9*, 1113−1122.
(45) Gomes, J. A. N. F.; Mallion, R. B. *Chem. Rev.* **2001**, *101*, 1349−1383.

Table 6. Aromatic Criteria[a]

	PDI	NICS(0)[b]	NICS(0)[c]	NICS(1)[b]	NICS(1)[c]
C_6H_6	0.103	−7.6	−7.9	−9.9	−10.1
	0.101[d]	−8.9[e]	−9.7[f]		
$[B_3N_3H_6]$		−2.1[e]			
$[B_3P_3H_6]$		−8.7[e]			
$[N_3P_3H_6]$	0.0156	+0.0	−1.2	+1.2	−0.1
			−2.2[g]		
$[N_3P_3F_6]$	0.0174	−5.1	−5.4	−2.4	−3.0
$[N_3P_3Cl_6]$	0.0179	−2.5	−4.1	−1.0	−2.7
$[N_3P_3Br_6]$	0.0176[h]	−1.7	−2.8	−0.4	−1.8
$[N_3P_3(CH_3)_6]$	0.0149	−1.9	−2.3	−0.4	−1.3
$[P_3N_3(CF_3)_6]$	0.0150[h]	−2.9	3.4	−0.7	−1.9
$[N_3P_3(NC_2H_4)_6]$	0.0127[h]	−5.0	−5.9	−2.7	−3.9
$[N_3P_3(O_2C_6H_4)_3]$	0.0163[h]	−3.8	−4.1	−1.3	−2.3
$[N_4P_4Cl_8]$	0.0085[i]				
$H[NPCl_2]_4H$	0.0118[j]				

[a] Values are averaged. [b] Using standard basis sets (see section 2). [c] Using a 6-31+G(d) basis set for all atoms. [d] From ref 44, calculated at the HF/6-31G* level. [e] From ref 42h, calculated using the IGLO method at the SOS-DFPT-IGLO level with Perdew−Wang-91 exchange correlation and the IGLO−III TZ2P basis set. [f] From ref 18a, calculated at the MP2/6-31G*//GIAO−SCF/6-31+G* level. [g] From ref 42g, calculated at the B3LYP/6-31G* level. [h] Using the 6-31G(d,p) basis set for all atoms to generate the AIMPAC input file. [i] δ(*P*−N−P−N, P−N−P−*N*). [j] δ(*A*−A−A−A, A−A−A−*A*), A = P or N, excluding the terminal N and P centers.

matic) or $[B_3P_3H_6]$ (modest aromatic character).[42h] Natural chemical shielding NCS analysis of the NICS values (see Supporting Information section S4) indicates that the largest contributions to the negative NICS values originate predominately from the non-Lewis-type delocalizations (negative hyperconjugation) of the N_{lp2} NBOs, with other contributions from the corresponding non-Lewis delocalization of the N_{lp1} NBOs and Lewis-type contributions from the σ_{PN} NBOs. These are countered by large positive Lewis-type contributions from the N_{lp1} NBOs. The presence of cyclic delocalization is further suggested by significant NLMO/NPA P−P bond orders and δ(N,N) values together with PDI values, although lower than benzene (ca. 0.1 vs 0.02). Significantly, a larger PDI value is calculated for $[N_3P_3Cl_6]$ (0.0179) than the corresponding 4-center delocalization indices in both the nonplanar $[N_4P_4Cl_8]$ (0.0085) and the noncyclic $H[NPCl_2]_4H$ (0.0118), indicative of significant enhancement of delocalization in $[N_3P_3Cl_6]$.

4. Conclusions

Natural bond order analysis of a range of phosphazenes has verified the important role negative hyperconjugation plays in the description of the valence unsaturated P−N bond. In these molecules, this interaction is mediated through the interaction of both in-plane and out-of-plane nitrogen lone-pair orbitals with σ^*_{PN} and σ^*_{PX} orbitals, respectively. However, while this bonding model is necessary for a more complete description of the bonding, ionic bonding appears to be the dominant bonding feature, with substantial P to N charge-transfer conferring significant ionic character to the P−N bond. Using NBO occupancies, negative hyperconjugation accounts for approximately 15% of the P and N valence electrons not involved in σ bonding, although with electron-withdrawing substituents, which enhance $N_{lp2} \rightarrow \sigma^*_{PCl}$ and $N_{lp1} \rightarrow \sigma^*_{PN}$ NBO donor−acceptor interactions, negative hyperconjugation plays a larger role, for example, 18% in $[N_3P_3Cl_6]$. Furthermore, variations in P−N bond length among the substituted cyclotriphosphazenes correlate well with the destabilization energy of their σ^*_{PN+PX} NBO deletions, encompassing the energetic importance of the negative hyperconjugation, suggestive of the important role these interactions play in the formation of strong P−N bonds. Significantly, unsymmetrical negative hyperconjugative bonding contributions were found to lead to P−N bond alternation. In particular, the observed bond length alternation in $[N_3P_3(NC_2H_4)_6]$ and the oligomeric phosphazene *cis,trans*-$H[NPCl_2]_4H$ could be rationalized in terms of unequal negative hyperconjugation contributions from substituent and ring lone pairs, respectively. The later provides a previously lacking and compelling explanation for the bond length alternation observed in some linear polyphosphazenes. It also appears that contributions from negative hyperconjugation build multiple-bond character into the P−N bond with minimal hindrance to bond rotation. Together, these results serve to reinforce Reed and Schleyer's perspective that chemical bonding in hypervalent molecules is dominated, not by valence d-orbital participation, but by ionic bonding and negative hyperconjugation.[7] Specifically in this case, low P_{3d} occupancies were found from the NPA analysis consistent with their primary role as polarization functions.[6]

Nucleus independent chemical shift values, especially for the more electronegative substituents, are suggestive of the presence of (weak) cyclic delocalization that originates from multiple-bond character derived from negative hyperconjugation. This suggestion is further suppored by para-delocalization indices. In particular, the index of $[N_3P_3Cl_6]$ is significantly enhanced in comparison to the corresponding 4-center indices of both the nonplanar $[N_4P_4Cl_8]$ and the noncyclic *cis,trans*-$H[NPCl_2]_4H$. Together, these results are suggestive of the fulfilment of some of the necessary aromaticity critera for the cyclotriphosphazenes, indicating their inclusion as potential "inorganic benzene" candidates, although further research is needed to consolidate this suggestion.

Acknowledgment. We thank the New Zealand Foundation for Research, Science and Technology for a Top Achiever Doctoral Fellowship (A.B.C). We are also grateful for access to the Helix parallel-computing facility (Massey University at Auckland) and the Linux computer cluster of Prof. A. E. Merbach (EPFL).

Supporting Information Available: Summary of preliminary geometry optimizations of $[N_3P_3Cl_6]$ using different model chemistries (Table S-1), optimized geometries of the molecules investigated in this investigation (Table S-2), selected topological properties (and short discussion, section S2), a natural resonance theory (NRT) analysis of $[H_2NPH_2]$, $[HNPH_3]$, and [HNPH] (section S3), and natural chemical shielding (NCS) data related to the ghost atoms used for the NICS analysis (Table S-5). This material is available free of charge via the Internet at http://pubs.acs.org.

IC0511266